5.1 Introduction

Since last decades, the gold nanoparticles (AuNPs) have played an important role in the various areas such as biosensing (Varun *et al*. 2017), catalysis (Shen *et al*. 2017), anticancer (Ramachandran *et al*. 2017), medicine (Ribeiro *et al*. 2017), electronics (Daniel and Astruc 2004), etc. AuNPs is synthesized through several routes like physical, chemical and biological where the physical and chemical routes suffered by the several environmental pollution issues, costly instrumentation and energy consumption while heating and stirring (Muthukumar *et al*. 2016). The principles of green chemistry have played a major role in biological (green) synthesis of AuNPs by involving green route using algae (Gonzalez-Ballesteros *et al*. 2017), fungi (Barabadi *et al*. 2017), bacteria (Ojo *et al*. 2016) and plants (Gonnelli *et al*. 2018). The green synthesis route has eliminated the need of hazardous chemicals, costly instrumentations and energy consumption.

Currently, plant extracts are being extensively used for the green synthesis of AuNPs due to more advantageous over other biological sources because of user-friendly, economically efficient, and environment-friendly in nature (Kumar *et al*. 2017a). It also does not require the aseptic conditions, and maintenance of microbial culture (Kumar *et al*. 2017b). Several authors have claimed the presence of phytochemicals such as tannins, flavonoids, terpenoids, proteins, hydrogenases, reductases etc in plant extract which acts as both reducing and stabilizing agent (Kumar *et al*. 2017c). Therefore, currently the plant extracts are being utilized broadly for the green synthesis of AuNPs. Recently, several plants like *Spinacia oleracea* (Ramachandran *et al*. 2017), *Actinidia deliciosa* (Naraginti and Li 2017), *Vetiveria zizanioides* (Swain *et al*. 2016), *Cacumen Platycladi* (Liu *et al*. 2017), have been used for the synthesis of AuNPs.

The plant extract mediated photoinduced green synthesis of AuNPs is proven to be more rapid, eco-friendly, and economically efficient which avoids the energy consuming processes like heating and stirring (Kumar *et al*. 2017a). There are several articles which have been published for the biosynthesis of AuNPs using sunlight induced route. Recently, we have published green synthesis of silver nanoparticles (AgNPs) using aqueous extract of *X. strumarium* (AEX) (Kumar *et al*. 2016a) and the current paper is aimed for the optimized synthesis of AuNPs using the same plant. In our previous study, we have also reported the photoinduced synthesis of AgNPs using aqueous extract of *Croton bonplandianum* (Kumar *et al*. 2017a), *Murraya koenigi* (Kumar *et al*. 2017b), *Erigeron bonariensis* (Kumar *et al*. 2016b), *Physalis angulata* (Kumar *et al*. 2017c), and *Euphorbia hirta* (Kumar *et al*. 2016c) through sunlight induced route.

The Xanthium strumarium (*compositae* family) is a common weed which is found throughout the tropical regions of India and commonly known as cocklebur (Kamboj and Saluja 2010). The phytochemical study corroborated the presence of several phytochemicals such as alkaloids, flavanoids, triterpenoids, terpenoids, tannin, saponin, quinone, protein and sugars (Farooq *et al*. 2014). In the present investigation, the AEX was utilized for the potential biosynthesis of AuNPs. The biosynthesis of AuNPs was optimized using one parameter at a time approach and effect of metal ion concentration on the shape and size of AuNPs was investigated through TEM analysis.

Thus obtained AuNPs was characterized through various modern characterizing techniques where the zeta potential study revealed the synthesis of negatively charged AuNPs (NC-AuNPs). The NC-AuNPs were investigated for its peroxidase-like catalytic activity in the presence of substrate like tetramethylbenzidine and H_2O_2 for the colorimetric

detection of H_2O_2. This is the first report on the peroxidase-like activity of NC-AuNPs synthesized from leaf extracts.

5.2 Materials and methods

5.2.1 Preparation of leaf extract

The preparation of leaf extract is discussed in chapter 3 section 3.2.1

5.2.2 Biosynthesis of NC-AuNPs

In order to synthesize NC-AuNPs, 3% AEX was added into 2 mL of 0.8 mM $HAuCl_4.xH_2O$ solution at neutral pH and exposed to sunlight. The sunlight intensity (Lux Meter) and the temperature (Thermometer) of the ambient environment were 68600 lux and 40 °C respectively. To avoid the fluctuation of sunlight intensity and temperature, all the synthesis reactions were carried out between 12.0 pm to 2.0 pm. To compare the effectiveness of the sunlight, the same reaction was also performed in dark condition which did not reveal the presence of any color change and sharp SPR band. Therefore, the NC-AuNPs synthesis and its optimization reaction were carried out in sunlight. The factors affecting the synthesis processes like exposure time, AEX dose % (v/v), and metal ion concentration were also optimized using one parameter at a time approach in the range of 0-40 min, 1% to 8% AEX dose and 0.4 mM to 3.2 mM respectively. After optimization at the above mentioned conditions, the optimum NC-AuNPs thus obtained was centrifuged at 15000 rpm for 15 min and then redispersed in UPW to eradicate the secondary metabolites and water soluble molecules. This process was repeated three times. The pellet of NC-AuNPs thus obtained was collected and used for the characterization purpose.

5.2.3 Experimental methodology

Primarily, the NC-AuNPs synthesis was confirmed by UV–visible spectrophotometer (Evolution 201, Thermo Scientific) in the range of 400 to 800 nm. The actively participated functional groups in the reduction of Au^{3+} to Au^{0} were confirmed by Fourier Transform Infrared Spectrophotometer (FTIR, Perkin Elmer Spectrum 100) in the range of 4000–400 cm^{-1}. The effect of different metal ion concentration on the crystallinity of the NC-AuNPs was investigated through X-ray Diffractometer (XRD) at $2\theta = 20°$ to 80° with the 6° min^{-1} of scanning rate and 0.02° of step size (Rigaku Miniflex II) having Cu Kα radiation source and Ni filter. Malvern Zetasizer (Malvern Instruments, Ltd.) was used to measure the zeta-potential of the AuNPs. The crystallinity of NC-AuNPs was also confirmed by the presence of concentric diffraction rings in Selected Area Electron Diffraction (SAED) pattern. The size and shape of the synthesized NC-AuNPs were studied by Transmission Electron Microscopy (TEM) carried out on TECNAI 20 G2-electron microscope operated at accelerating voltage 200 kV. The EDX equipped with TEM confirmed the purity and elemental constituents of NC-AuNPs. The X-Ray Photoelectron Spectroscopy (XPS, AMICUS, Kratos Analytical, A Shimadzu) as X-ray source with Mg Kα (1253.6 eV) was used to confirm the speciation of biosynthesized NC-AuNPs. Thus synthesized AuNPs possessed excellent peroxidase-like mimetic which was applied in the colorimetric detection of H_2O_2 and its detail procedure is given in chapter 2 under section 2.5

5.3 Results and discussion

The change in color from light yellow to dark purple was the primary indication of the synthesis of NC-AuNPs. This change in color was due to the surface plasmon resonance

(SPR) which produced through collective oscillations of free conduction electrons and caused to change in color of the reaction mixture (Kumar *et al*. 2017a). It was noticed that the reaction mixture of AEX and $HAuCl_4.xH_2O$ keeping in sunlight, showed an instant color change and sharp SPR band at 542 nm within few min of sunlight exposure which was due to the surface plasmon resonance of AuNPs having λ_{max} values in the range of 500-600 nm (Reddy *et al*. 2012).

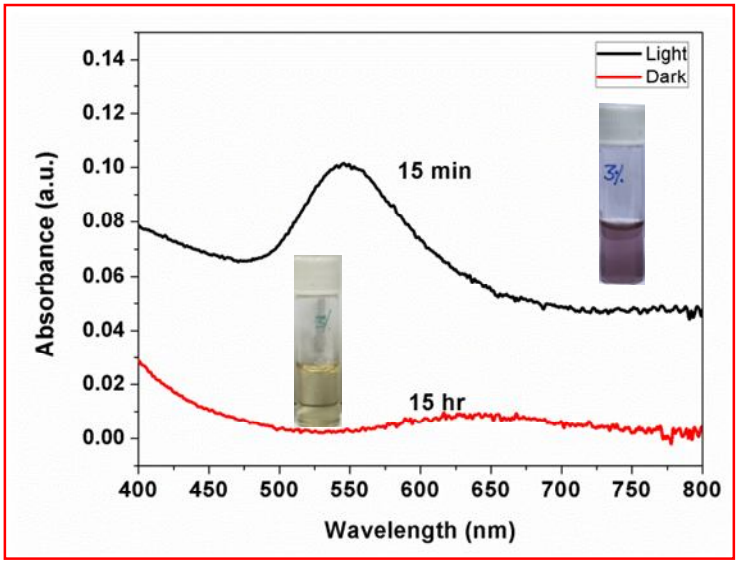

Figure 5.1 UV-visible spectra of NC-AuNPs in sunlight and dark condition with corresponding change in color

The change in color and presence of SPR band advocated the rapid synthesis of NC-AuNPs in sunlight. Whereas the reaction mixture keeping in dark condition did not reveal any change in color which confirmed that dark condition was not competent to synthesize NC-AuNPs even after 15 hrs of incubation **(Fig. 5.1)**. This time lag clearly indicated the rapid synthesis of NC-AuNPs in sunlight as compared to dark condition.

5.3.1 Optimization of the process parameters

5.3.1.1 Sunlight exposure

At the very first, the sunlight exposure time required to reach to the extent of equilibrium level of the proceeding reaction was optimized. This optimization was performed by withdrawing the fixed amount of aliquots (100 µL diluted in 3 mL UPW) from the exposed reaction mixture at each 5 min of interval and subsequently measuring the UV-visible spectra. The exposed reaction mixture revealed that with the increase of exposure time, the pattern of darkening of the color towards dark purple also increased (**Fig. 5.2A-H**). It was observed that the reaction mixture of 1% AEX dose exposed to sunlight, neither showed any color change nor presence of any SPR band. The absence of color and SPR band clearly indicated that the nuclei formed were smaller than critical nuclei and redissolved in the reaction mixture, therefore failed to nucleate to form NC-AuNPs (Peng and Yang 2009, Bøjesen and Iversen 2016). Thereafter, the intensity of the SPR band was found to be increased continuously at each 5 min of exposure time up to 30 min. Further, on increasing the exposure time, the intensity of the SPR band ceased to increase. This pattern was also found to be same for 2% and 3% AEX. The pattern of increase in intensity of SPR band corroborated the increased synthesis of NC-AuNPs whereas further no development of intensity of SPR band confirmed the establishment of the equilibrium (Kumar *et al*. 2017c). Thereafter, an interesting phenomenon of changing of the SPR pattern towards a different pattern was observed while screening from 4% to 7% AEX (Kumar *et al*. 2017b). Although, the intensity of the SPR band increased up to 6% AEX, it continued to broader with continued flattening of longer wavelength head with the proceeding of sunlight exposure time. The continued broadening and steepening of SPR band of longer wavelength head

advocate to the synthesis of larger anisotropic NC-AuNPs due to agglomeration (Kelly *et al.* 2003).

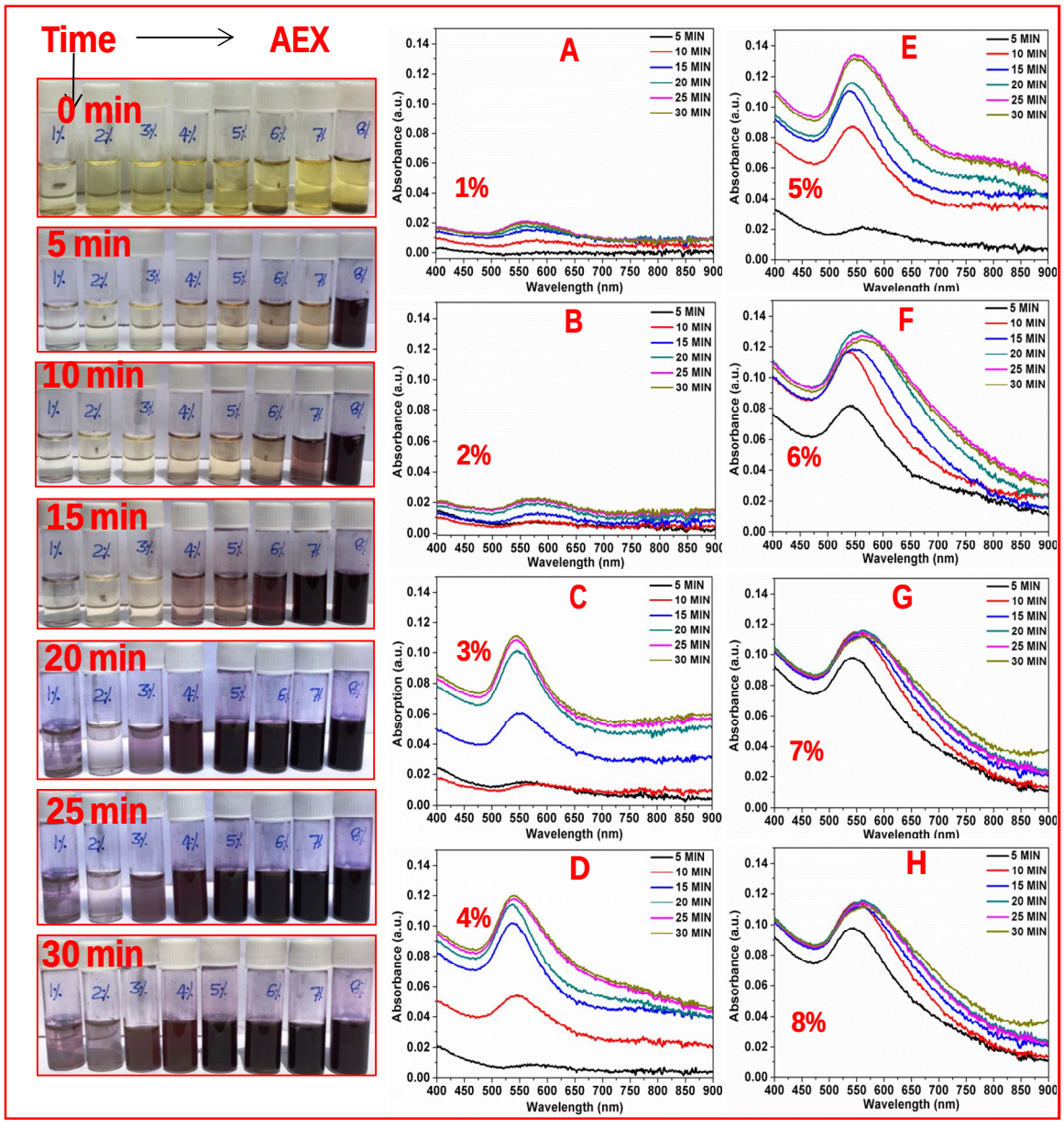

Figure 5.2 UV–visible absorption spectra of AuNPs synthesis using different AEX inoculums doses at 1% to 8% from A – H respectively and their corresponding increase in intensity and color change pattern with the proceeding of time from 5 to 30 min (conditions; 0.8 mM $HAuCl_4.xH_2O$ concentration, 5 to 30 min sunlight exposure time and 1% to 8% AEX inoculums dose)

5.3.1.2 AEX inoculums dose

The different pattern of SPR bands were produced by different AEX inoculums doses form 1% to 8% at constant exposure time of 30 min which are shown in **Figure 5.2A-H**. The pattern of the SPR band revealed the increased synthesis of NC-AuNPs with the increase in AEX inoculums dose upto 3%. The SPR band produced by 1% and 2% AEX inoculums doses were less steeper which suggested the synthesis of fewer numbers of NC-AuNPs (Kumar *et al*. 2016a). Further, on increasing the AEX dose by to 3%, the most sharp and intense SPR band was produced which indicated that it was the most suitable inoculums dose for the optimum synthesis of NC-AuNPs. Thereafter, SPR band produced through 4%, 5%, 6%, 7% and 8% AEX continued to be broader and steeper. The broadening and the flattening of SPR band from 4% to 8% AEX indicated the synthesis of larger sized anisotropic NC-AuNPs due to the overgrowth (Kumar *et al*. 2016a). The SPR band of each AEX inoculums doses revealed that the use of higher inoculums doses resulted in the faster development of the sharp SPR in first 5 min of exposure which was also strengthened from the development of the color. These interesting results were due to the burst nucleation at higher doses which resulted in the formation of large number of nuclei greater than critical nuclei. These nuclei coalesced to form NC-AuNPs sooner than lower inoculums doses. But due to absence of sufficient amount of capping agent, the formed NC-AuNPs no longer remained smaller and agglomerated to form the larger NC-AuNPs. Hence; the intensity of the SPR band started to decrease with the increase in AEX doses. Mie theory states that the diameter of the nanoparticles depends on the intensity and the position of the SPR band (Kumar *et al*. 2017a). Therefore, 3% AEX inoculums dose at 30 min of sun light exposure was considered as the optimum inoculums dose for the synthesis of NC-AuNPs.

5.3.1.3 $HAuCl_4.xH_2O$ concentration

After optimizing the sunlight exposure time and AEX inoculums doses, different concentration of $HAuCl_4.xH_2O$ from 0.4 mM to 3.2 mM were optimized at constant 3% of AEX inoculums dose and 30 min of sunlight exposure time for the optimum synthesis of NC-AuNPs. It is obvious from the **Figure 5.3A-H** that the color of reaction mixtures of each $HAuCl_4.xH_2O$ continued to be darker with the passes of exposure time from 5 to 30 min. It is well established fact that the size of NC-AuNPs is related with the color of NC-AuNPs solution which was also confirmed by TEM analysis. The TEM analysis confirmed the increase in average size of the NC-AuNPs from 11.1 to 99.49 nm with the increase in $HAuCl_4.xH_2O$ concentration from 0.4 mM to 2.8 mM (**Fig. 5.4A-G**). Thus it is confirmed that the size of the NC-AuNPs is governed by the color of NC-AuNPs solution (Bastus *et al*. 2014). While screening, it was observed that different concentrations of $HAuCl_4.xH_2O$ from 0.4 to 3.2 mM showed a diverse pattern of SPR bands. The pattern revealed that firstly, the intensity of SPR band increased from 0.4 mM to 1.2 mM. This increase in intensity advocated the increased synthesis of NC-AuNPs which was strengthened by the TEM results (**Fig. 5.4A-C**). Thereafter, it started to broaden with continuous decrease in intensity up to 3.2 mM which was due to the formation of larger NC-AuNPs because of agglomeration. This was also confirmed by the TEM analysis (**Fig. 5.4A-H). Figure 5.3A** revealed that the color and SPR bands produced by 0.4 mM $HAuCl_4.xH_2O$ from 5-30 min were much lighter and lesser intense respectively. The light color of the solution and lesser intense SPR band indicated towards the lesser synthesis of NC-AuNPs as showed by the TEM image (**Fig 5.4A**).

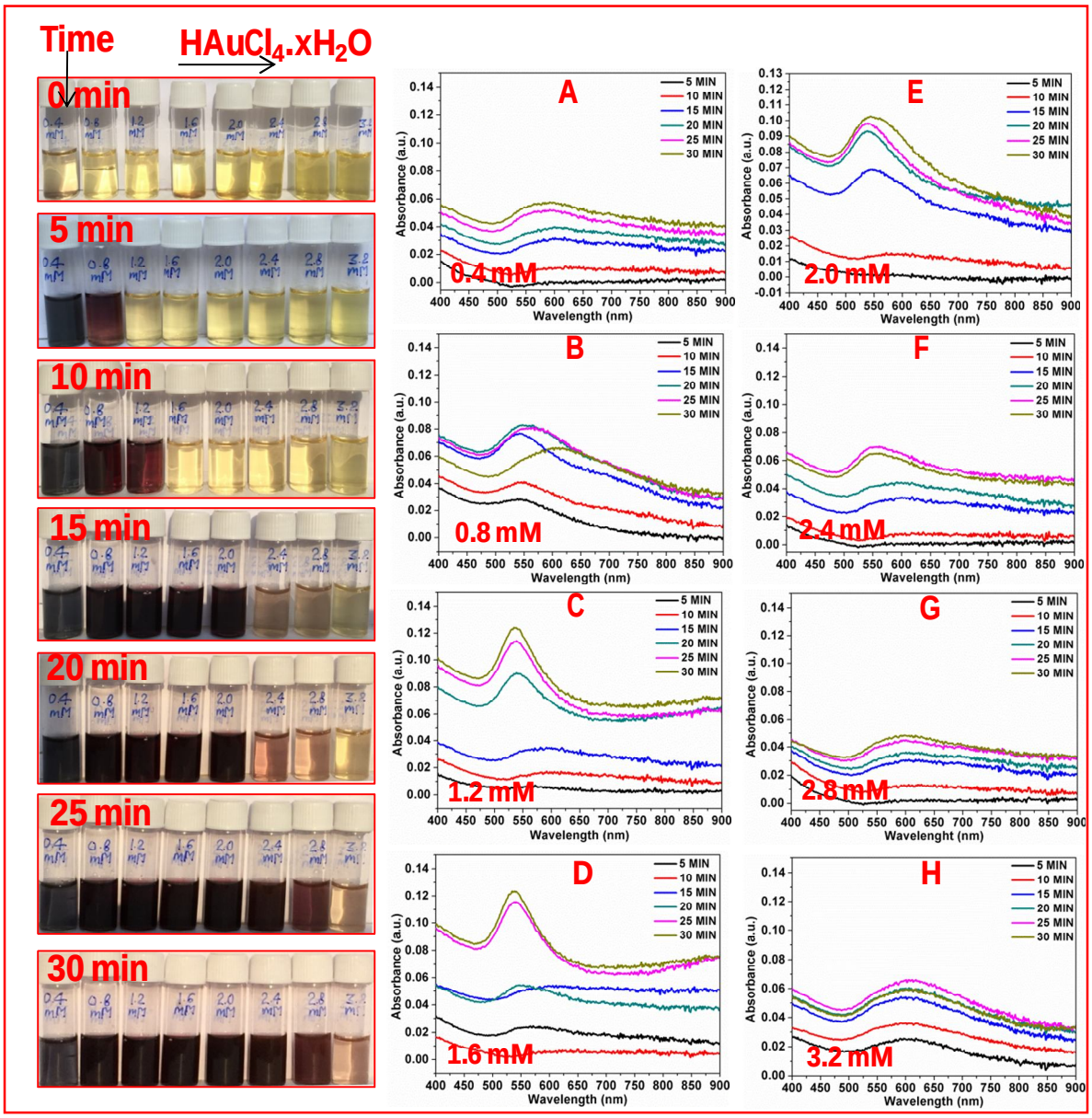

Figure 5.3 UV–visible absorption spectra of AuNPs synthesis using $HAuCl_4.xH_2O$ concentration from 0.4 mM – 3.2 mM (A – H respectively) using 3% AEX inoculums dose and their corresponding increase in intensity and color change pattern with the proceeding of time from 5 to 30 min (conditions; 3% AEX inoculums dose and 5 to 30 min sunlight exposure time and 0.4 mM – 3.2 mM $HAuCl_4.xH_2O$ concentration)

After that it was found that the color and intensity of the SPR band of 0.8 mM, and 1.2 mM continued to be increased at each time interval. This indicated that by increasing the $HAuCl_4.xH_2O$ concentration, the synthesis of NC-AuNPs increased with increased average size which was also confirmed by TEM analysis (**Figure 5.4B-C**) (Lee *et al*. 2016). **Figure 5.3D-H** also indicated that the SPR band intensity of 1.6 mM, 2.0 mM, 2.4 mM, 2.8 mM and 3.2 mM continued to be decreased with continuous broadening which might be due to overgrowth as can be seen from the TEM images (**Figure 3D-H)**. It is a well established fact that the generated nuclei having low concentration of precursor monomers form spherical/pseudospherical nanoparticles. The anisotropic nanoparticles are formed when the generated nuclei having high concentration of precursor monomers. It was observed that on increasing the $HAuCl_4.xH_2O$ concentration, the formation of anisotropic NC-AuNPs like trigonal, hexagonal, pentagonal shaped increased due to increased monomer concentration as shown in **Figure 5.4 D-H** (Thanh *et al*. 2014). Therefore, in order to get smaller and large number of NC-AuNPs with controlled growth and smaller size, 1.2 mM $HAuCl_4.xH_2O$ concentration at 3.0% AEX and 30 min exposure time was chosen as optimal condition for the current study.

5.3.2 Mechanism involving NC-AuNPs formation

The reported phytochemical constituents of the *X. strumarium*, Ferric chloride test, Folin Ciocalteu's method, photomediated synthesis of NC-AuNPs and FTIR analysis of TA, AEX, pre-annealed NC-AuNPs and post-annealed NC-AuNPs inspired us to propose a mechanism of NC-AuNPs synthesis through AEX. Although, the presence of diverse variety of phytochemicals present in the AEX may reduce the Au^{3+} in different way but due to presence of prominent quantity of tannin, we have proposed a stepwise reduction of Au^{3+} into

Au^0 using this as a reducing agent. For the synthesis purpose, the AEX was mixed with the aqueous solution of $HAuCl_4.xH_2O$, where the OH group of polyphenolic compound (tannin) present in AEX formed the Au^{3+}/AEX complex by binding with Au^{3+}. From the results it is obvious that the synthesis of NC-AuNPs is photo-mediated.

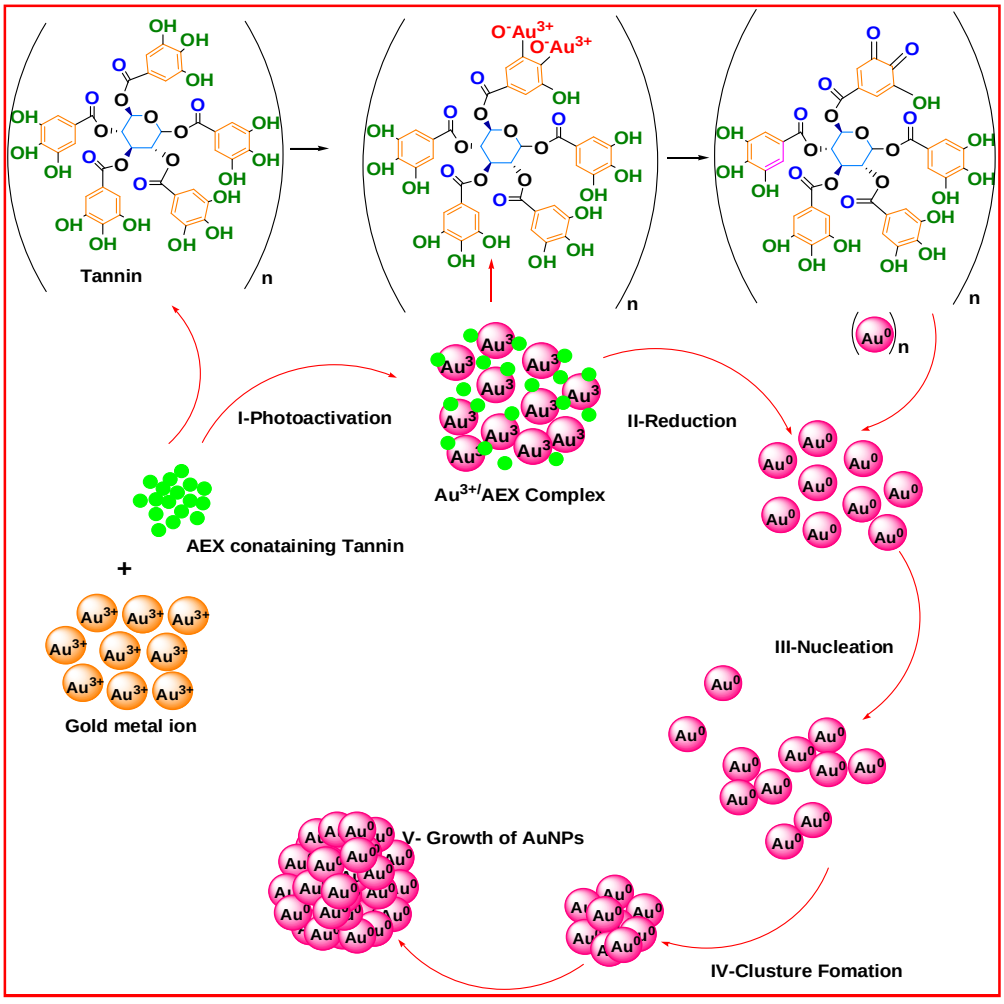

Scheme 5.1 The scheme showing the various steps of AuNPs synthesis by involving the enol form of 'n' number of polyphenolic groups of 'n' number of tannin present in AEX which formed complex (AEX/Au^{3+}) with Au^{3+} and further reduced the n[Au^{3+}] to n[Au^0] by the hydrated electrons released from the debonding of O-H bond. The n[Au^0] formed AuNPs after simultaneous nucleation, cluster formation and further growth

The first step of NC-AuNPs synthesis is the photo-activation of Au^{3+}/AEX complex which involved the release of hydrated electrons by debonding of OH group of AEX after absorbing the photons of light (Yang *et al*. 2015, Zhou *et al*. 2014, Pal and Pal 1999). Further, the electron thus released played an important role in the reduction of Au^{3+} to Au^0 in second step (Sakamoto *et al*. 2009). This continued reduction of Au^{3+} to Au^0 led to the increase in Au^0 concentration. Thus increased concentration of Au^0 started to nucleate and formed the crystal nuclei after exceeding the critical supersaturation level in step third. Thereafter, the formation of crystal nuclei was followed by the decrease in the concentration of Au^0 atoms below to the level of critical supersaturation where A^0 aggregated to form nanoclusters in step fourth. Finally, in fifth step, the formed nanoclusters finally grew into NC-AuNPs as can be seen from **Scheme 1.3** (Tran and Nguyen 2011).

The photosensitive nature of the polyphenolic compounds present in AEX strengthened the fact of photoinduced synthesis of NC-AuNPs which easily donated the electrons for the reduction of Au^{3+} to Au^0 (Gade *et al*. 2014). The above fact was also confirmed by the FTIR analysis which illustrated the major role played by $–NH_2$ and –OH groups in synthesis and stabilization of NC-AuNPs. The Schematic representation of (I) photoactivation of Au^{3+}/AEX complex, (II) reduction of Au^{3+} to Au^0 by involving n(OH) of n(tannin) present in AEX, (III) nucleation, (IV) to form nanocluster (V), and by further growth formation of NC-AuNPs is shown in **Scheme 5.1.**

5.3.3 Characterization

The optimized NC-AuNPs thus obtained was characterized through several modern characterizing techniques such as HR-TEM, SAED, XRD, and XPS analysis. In order to tune the shape and size of the NC-AuNPs, the concentrations of $HAuCl_4.xH_2O$ were varied from

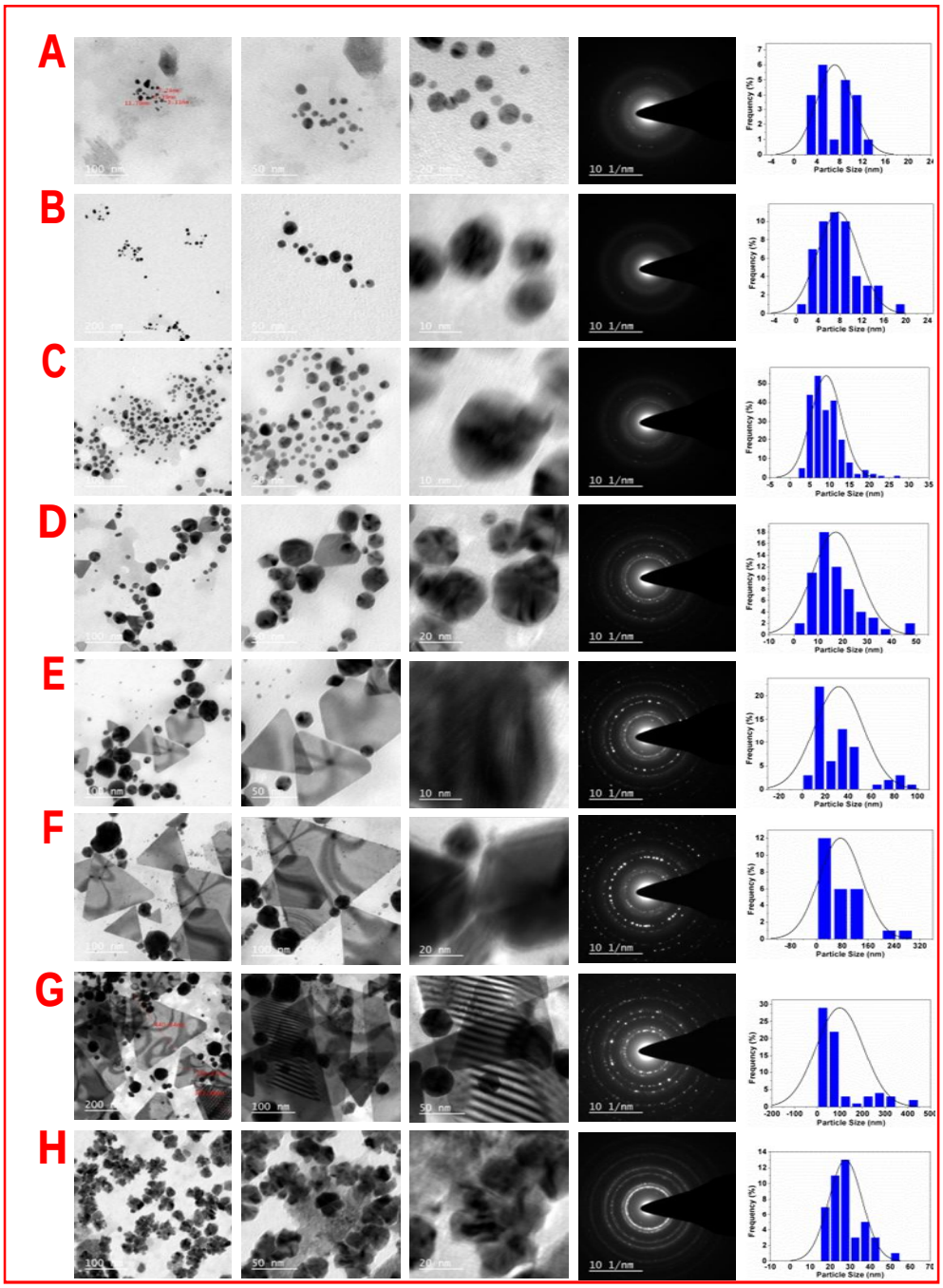

Figure 5.4 HR-TEM images of AuNPs synthesized from different $HAuCl_4.xH_2O$ concentration (0.4 mM to 3.2 mM) from A to H at different magnifications, their corresponding SAED pattern and histogram showing the crystalline nature of AuNPs and size distribution respectively

0.4 mM to 3.2 mM and the NC-AuNPs thus synthesized were investigated through HR-TEM analysis. **Figure 5.4A-H** represented the HR-TEM images of NC-AuNPs produced from 0.4 mM to 3.2 mM at different magnifications. The HR-TEM images of 0.4 mM at different magnification corroborated the discrete distribution of very less number of spherical NC-AuNPs with smaller sized. Thus obtained result was in accordance with the SPR band intensity and color of the reaction mixture. The distribution of NC-AuNPs size obtained from 0.4 mM is shown by histogram which revealed that NC-AuNPs range from 2.5 nm to 20.5 nm with average size 11.1 nm. The TEM images of 0.8 mM indicated the presence of larger number of spherical shaped NC-AuNPs and the corresponding histogram revealed that NC-AuNPs ranged from 1.8 nm to 18.5 nm with the average size 7.6 nm. The further increase in concentration by 1.2 mM corroborated the increased number of spherical NC-AuNPs in the range of the 3.5 nm to 22 nm with the average size of 9.1 nm as shown by histogram. The TEM images of 1.6 mM showed that the formation of anisotropic NC-AuNPs like trigonal and hexagonal started to develop. The NC-AuNPs ranged of 5 nm to 27 nm having average size 17.1 nm. The formation of trigonal and hexagonal NC-AuNPs with larger sized continued to be increase upto 2.8 mM. The anisotropic NC-AuNPs produced from 2.0 mM, 2.4 mM, and 2.8 mM ranged from 10 nm to 93 nm, 6 nm to 149 nm, and 17 nm to 440 nm with an average size 31.8 nm, 74.4 nm and 99.5 nm respectively. The NC-AuNPs produced from 3.2 mM showed an extraordinary result. It revealed the formation of flower shaped NC-AuNPs ranging from 15 nm to 41 nm with average size 27.6 nm. In summary, it was observed that the average size of the NC-AuNPs and the synthesis of larger sized anisotropic NC-AuNPs increased on increasing the $HAuCl_4.xH_2O$ concentrations (**Fig. 5.5A).** The

increase in average size of NC-AuNPs with the increase of $HAuCl_4.xH_2O$ concentrations showed a good linear relationship having $R^2 = 0.96$ (**Fig. 5.5B)**.

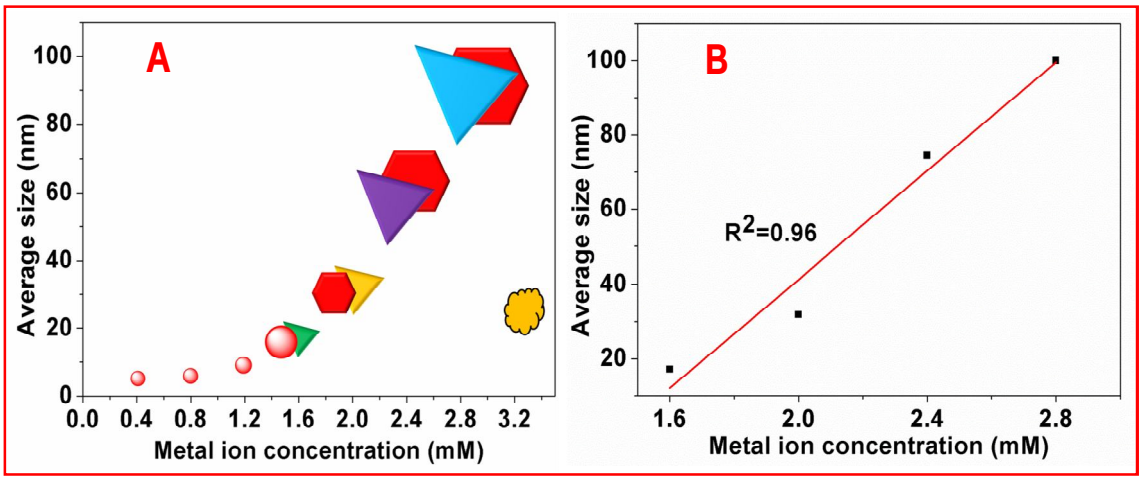

Figure 5.5 (A) Graphical representation of change in average size and shapes of AuNPs with the increase in $HAuCl_4.xH_2O$ concentration from 0.4 mM to 3.2 mM, (B) linear relationship between the average size and corresponding $HAuCl_4.xH_2O$ concentration

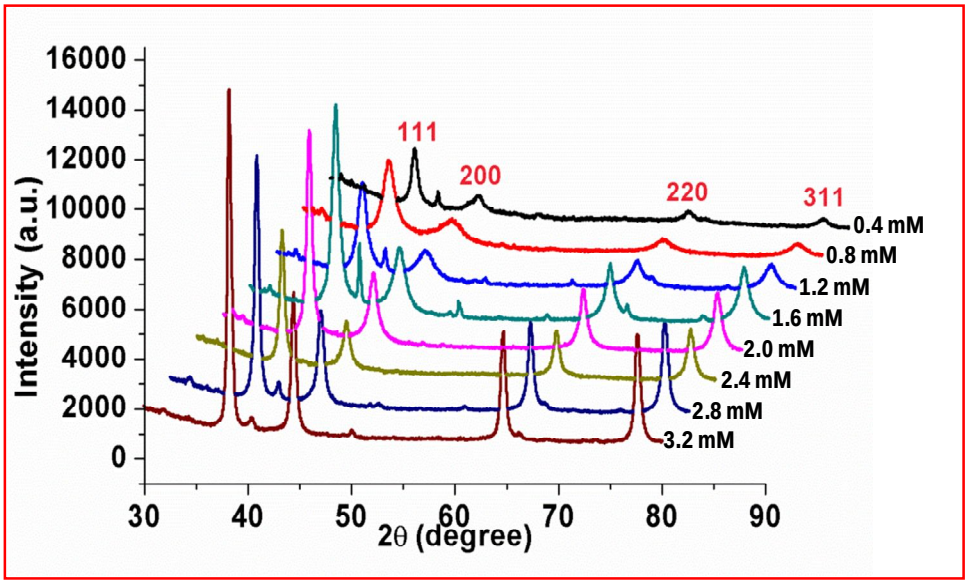

Figure 5.6 X-ray diffraction patterns of AuNPs obtained from different $HAuCl_4.xH_2O$ concentration (0.4 mM -3.2 mM)

The SAED pattern obtained from each $HAuCl_4.xH_2O$ concentrations showed the presence of circular ring which suggested the crystalline nature of the NC-AuNPs except of 0.4 mM and 0.8 mM which did not show any circular ring.

The synthesized NC-AuNPs from 0.4 to 3.2 mM were further characterized through XRD to investigate the crystalline nature and data were collected in the 2θ range of $30° \leq 2\theta \leq 80°$ with step size 0.02° and scan rate 6° min^{-1}. **Figure 5.6** showed the characteristic XRD patterns of NC-AuNPs from 0.4 to 3.2 mM which revealed the presence of similar diffraction peaks at the same $2\theta = 38.1^{\circ}$, 44.3°, 64.6° and 77.6°. The peaks were well matched with standard diffraction data with those reported for gold by Joint Committee on Powder Diffraction Standards (JCPDS) file no: 040784 and attributed to (111), (200), (220) and (311) Bragg reflections respectively. These Bragg reflections corresponded to the crystalline planes of the face centered cubic (fcc) crystal lattice of metallic gold.

The type of functional groups involved in the reduction and capping of NC-AuNPs were investigated by the FTIR analysis. The presence of polyphenolic compounds like tannin, flavonoids and terpenoids etc. in AEX were already been reported by several authors (Kamboj and Saluja 2010, Farooq *et al.* 2014). In our study, the presence of polyphenolic compound like tannin was also tested by Ferric chloride test and further the total polyphenolics were quantified too by Folin-Ciocalteu's Method which is discussed in detail in chapter 2 section 2.3.2 Therefore, the FTIR spectrum of AEX was compared with the FTIR spectrum of pure tannic acid (TA). The FTIR spectra of pure TA, AEX, pre-annealed NC-AuNPs and post-annealed NC-AuNPs are shown in **Fig. 5.7**. The peaks present in the FTIR spectrum of AEX were matched with the peaks present in pure TA to confirm the presence of tannin like moieties in AEX. The major functional groups involved in the

biosynthesis of NC-AuNPs were investigated by comparing the FTIR spectrum of AEX with the FTIR spectrum of pre-annealed NC-AuNPs. The phytochemicals involved in the capping of the NC-AuNPs was also identified by comparing the FTIR spectrum of post-annealed NC-AuNPs with the FTIR spectrum of pre-annealed NC-AuNPs.

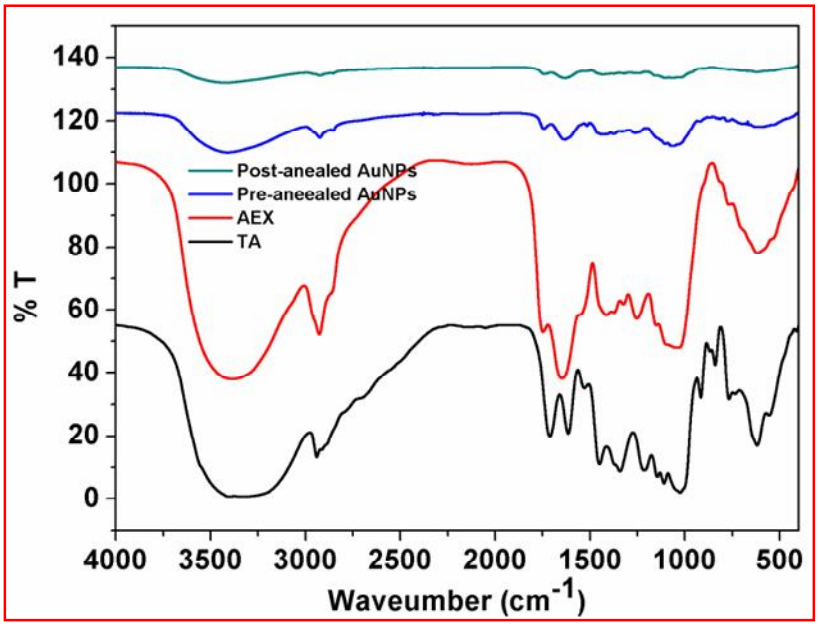

Figure 5.7 FTIR spectra of pure TA, AEX, pre-Annealed and post-annealed AuNPs showing the involvement of various functional groups for the synthesis and stabilization of AuNPs

The FTIR analysis of pure TA showed the presence of characteristics band at 3397 cm^{-1} 2932 cm^{-1}, 1757 cm^{-1} 1643 cm^{-1}, 1423 cm^{-1} 1252 cm^{-1}, 1047 cm^{-1} and 617 cm^{-1} which corresponded to the presence of υ_s of OH, υ_s of C=C-H, υ_s of C=O, υ_b of N-H, υ_s of C=C, υ_s of O-C, υ_s of C-O and υ_b, bending vibration respectively (Kumar *et al*. 2017a). It was observed that the FTIR spectrum of the AEX showed the presence of similar band as that of TA which advocated the presence of tannin in AEX. The presence of tannin in AEX was also

strengthened by $FeCl_3$ test which showed dark green color (discussed in chapter 2 in section 2.3.2).

The FTIR analysis of the pre-annealed NC-AuNPs revealed the presence of similar characteristic bands as present in FTIR analysis of AEX except few bands with diminished and shifted which advocated the important role of tannin present in the synthesis of the NC-AuNPs. Both the spectra showed a shifting in following peaks: from 3387 to 3411 cm^{-1} (υ_s of OH of the polyphenolic compounds and υ_s of NH of the proteins) and 1650 to 1638 cm^{-1} (υ_s of C=C) (Huang *et al*. 2010). The peak present at 2929 cm^{-1} (υ_s of C=C-H), 1754 cm^{-1}(υ_s of CO), 1411 cm^{-1} (υ_s of C=C), 1053 cm^{-1} (υ_s of C-O) and get diminished whereas the peak present at 617 cm^{-1} (υ_B, bending vibration) completely disappeared. These results indicated the important role of hydroxyl, carboxyl, amino and amide groups present in AEX in the synthesis of NC-AuNPs. When the FTIR analysis of post-annealed NC-AuNPs was carried, it showed that the peaks were completely diminished which advocated the loss of biological molecules adhered at the surface of NC-AuNPs while stabilization.

The elemental analysis of NC-AuNPs was performed using XPS. **Figure 5.8A** showed the wide scan spectrum of NC-AuNPs which exhibited the presence of Au 4f, C 1s, and O 1s peaks. These peaks indicating the presence of Au, C, and O as a chief element present in the sample. The presence of C and O strongly advocated the involvement of biological molecules in the stabilization of the NC-AuNPs. The Au 4f core level spectrum of NC-AuNPs is shown in **Figure 5.8B** which revealed the presence of two peaks at 86.6 and 89.3 eV corresponding to the binding energies of Au $4f_{7/2}$ and Au $4f_{5/2}$ respectively. The splitting of the 3d doublet of Au was found to be 3.7 eV which strengthened the formation of pure metallic (Au^0) (Pogacean *et al*. 2015).

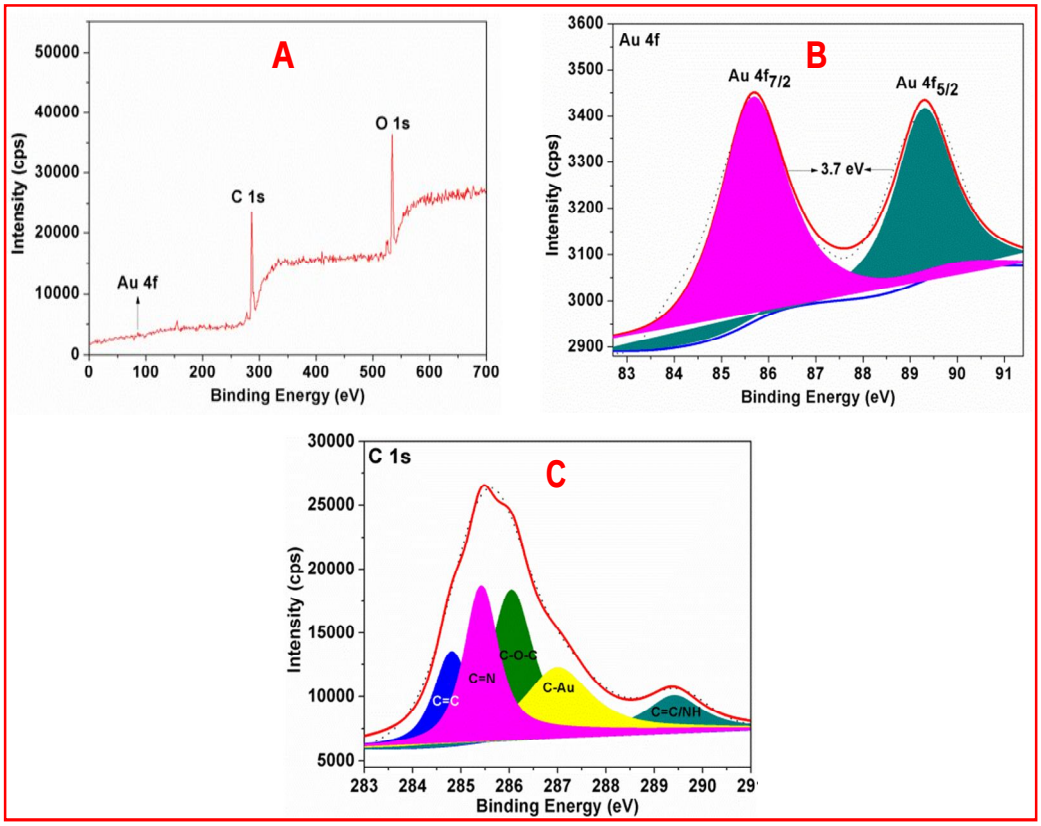

Figure 5.8 XPS spectra of AuNPs (A) Wide scan spectra, (B) Au 4f spectrum, (C) C 1s spectrum

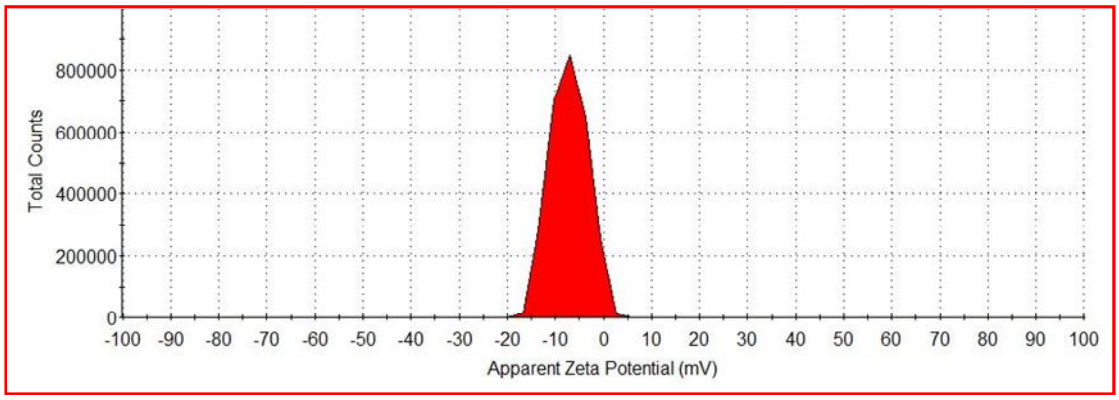

Figure 5.9 Zeta potential showing the negatively charged surface of AuNPs

Figure 5.8C represented the core level C 1s spectrum having Gaussian peaks at 284.9 eV (C=C), 285.5 eV (C=N), 286.30 eV (C–OH), 287.8 eV (C=O/C–Au), 289.98 eV (O–C=O).

The zeta potential study indicated that the surface of the AuNPs were negatively charged (-7.4 mV) which exhibited good stability in suspension (**Fig. 5.9**).

5.3.4 Peroxidase-like activity of NC-AuNPs

To investigate the peroxidase-like activity of the AEX synthesized negatively charged NC-AuNPs, the catalysis of TMB, a peroxidase substrate was evaluated in the presence of H_2O_2 to produce a blue color. For this, AEX synthesized NC-AuNPs was added into the TMB+H_2O_2 system and observed that, the reduced TMB (colorless) changed into oxTMB with the development of blue color. This blue color was due to the charge-transfer complex of the parent diamine and the diimine oxidation products having two absorption maxima at 370 nm and 652 nm (Guo *et al*. 2015) (**Scheme 5.2**).

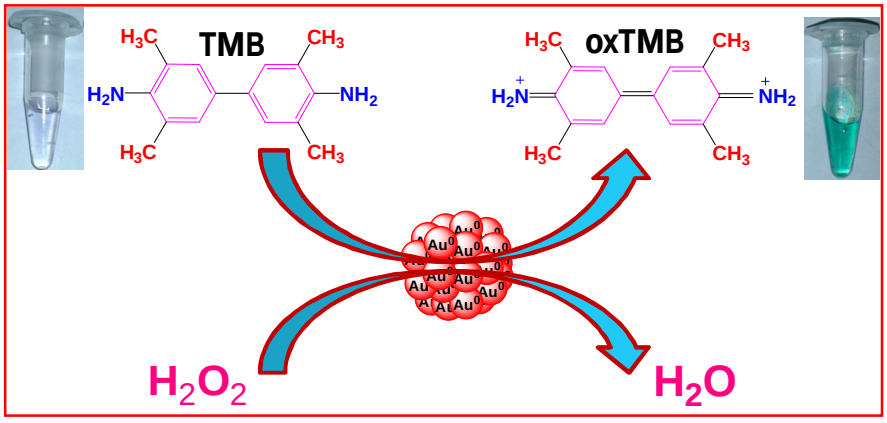

Scheme 5.2 Schematic illustration of peroxidase-like activity of AEX synthesized NC-AuNPs

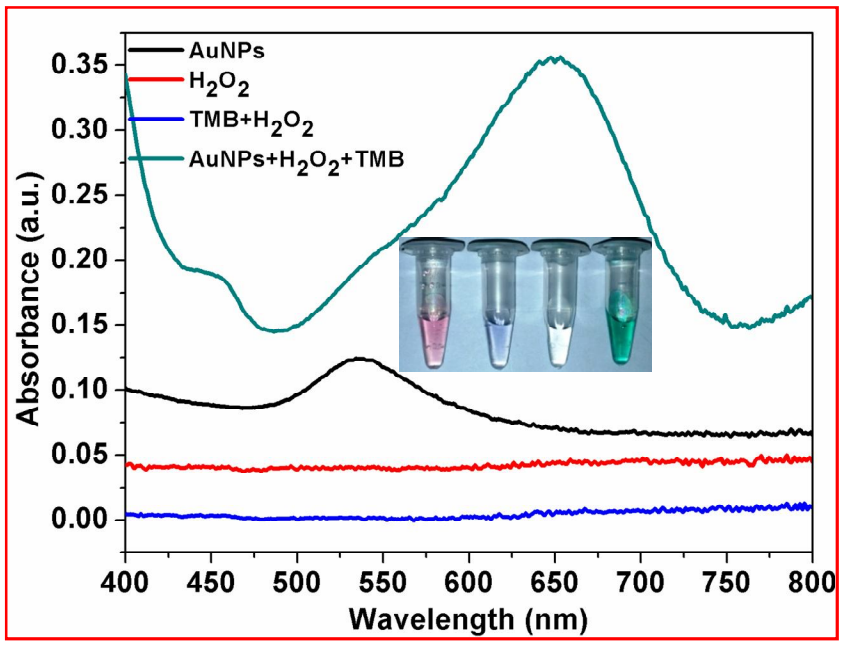

Figure 5.10 UV-visible spectra of NC-AuNPs, H_2O_2, TMB+H_2O_2, and NC-AuNPs+TMB+H_2O_2 system and their corresponding digital images

Figure 5.10 showed the UV-visible spectra of NC-AuNPs, TMB, TMB+H_2O_2, and NC-AuNPs+TMB+H_2O_2. The figure clearly revealed that NC-AuNPs, TMB, and TMB+H_2O_2, neither developed blue color nor any characteristic absorbance at 652 nm except NC-AuNPs+TMB+H_2O_2 system. It can be concluded that the colorless TMB+H_2O_2 system produced blue color only in the presence of NC-AuNPs. These results indicated the peroxidase-like activity of AEX synthesized negatively charged NC-AuNPs.

5.3.5 Optimization of factors affecting the peroxidase-like activity

After the successful establishment of peroxidase-like activity of AEX synthesized negatively charged NC-AuNPs, the different variables affecting the catalytic activity of natural enzyme like incubation time, pH, temperature and concentration were optimized to obtain the optimum results. The results showed that the catalytic activity of NC-AuNPs was

also dependent on the pH, temperatures and concentrations of TMB and H_2O_2 like natural enzymes.

The incubation time plays a very important role in chromogenic substrate based reactions to achieve the maximum absorbance at 652 nm. Therefore, the incubation time was optimized by regular monitoring the change in absorbance of NC-AuNPs+TMB+H_2O_2 system at each 5 min interval of time via UV-visible spectrophotometer.

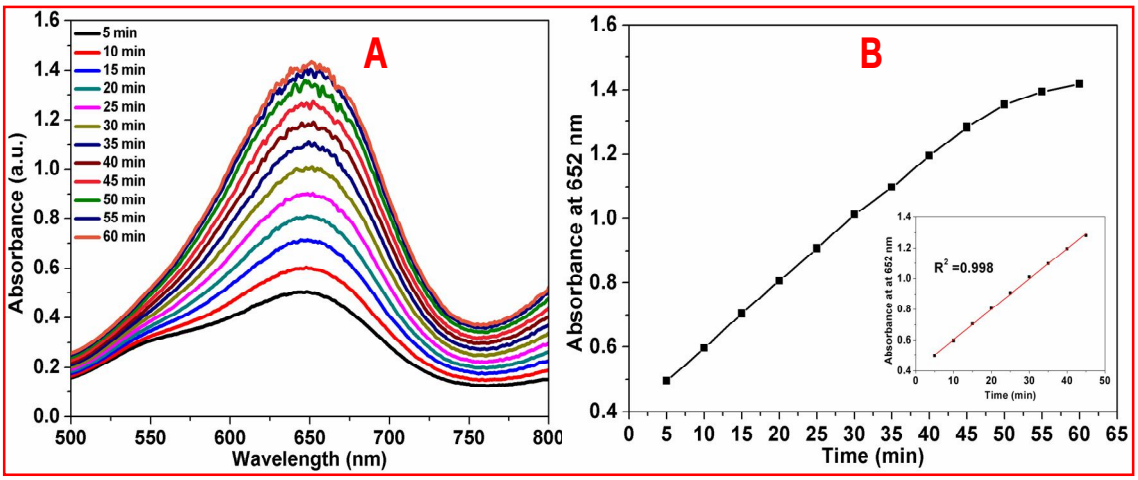

Figure 5.11 Peroxidase-like activity of NC-AuNPs at different (A) time interval using 50 µL of 1 mM TMB, 50 µL of 0.5 mM H_2O_2 and 50 µL of NC-AuNPs in 200 µL of 0.2 M NaAc buffer at constant pH 4 and temp 40 ^oC, (B) relationship between absorbance and incubation time with inset calibration plot showing the linear relationship between 5-54 min with R^2 = 0.998

It was observed that the intensity of the developed color from light blue to dark blue and absorbance at 652 nm increased on increasing the incubation time upto 60 min. Thereafter no significant change in color and absorbance was noticed (**Figure 5.11A**). Therefore, for obtaining the optimum peroxidase-like activity of NC-AuNPs, all the reaction systems were incubated for 60 min. The calibration plot of increase in absorbance vs

incubation time showed a good linear relationship in the range of 5 - 45 min with $R^2 = 0.998$ (**Fig. 5.11B**).

The peroxidase-like activity of NC-AuNPs at different pH range of 1-10 in 200 µL of 0.2 M NaAc is shown in **Figure 5.12A.** From the figure it is obvious that the peroxidase-like activity of NC-AuNPs was higher in acidic condition comparatively neutral and basic conditions with maximum activity at pH 4. Further, on increasing the pH beyond 4, it was observed that the peroxidase-like activity NC-AuNPs decreased and become negligible at higher pH. This interesting phenomenon was due to the decomposition of H_2O_2 into H_2O and O_2 rather $OH^{\bullet}$ radical (Feng *et al*. 2017).

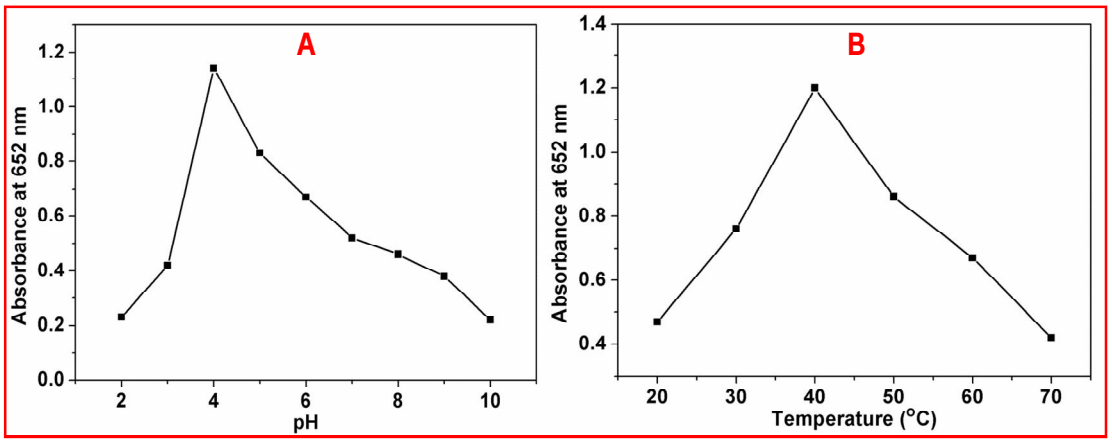

Figure 5.12 Peroxidase-like activity of NC-AuNPs at different (A) pHs ranging from 2 – 10 at 37 ^{o}C, and (B) temperatures ranging from 20 – 70 ^{o}C at pH 4 using 50 µL NC-AuNPs + 50 µL of 1 mM TMB + 50 µL H_2O_2 of 0.5 mM in 0.2 M NaAc buffer solution

Figure 5.12B represented the peroxidase-like activity of NC-AuNPs at different temperatures ranging from 20 ºC - 70 ºC. The figure revealed that NC-AuNPs showed the optimum peroxidase-like activity at temp 40 ºC which decreased on further increase in temperature. The reason behind the decrease in activity at higher temperature was the

agglomeration of NC-AuNPs which hindered the transfer of electron (Feng *et al*. 2017). Similarly, the other parameters affecting the peroxidase-like activity like NC-AuNPs amount and TMB concentration were also optimized using the same reaction system at constant incubation time of 60 min, pH 4, and temp 40 ºC.

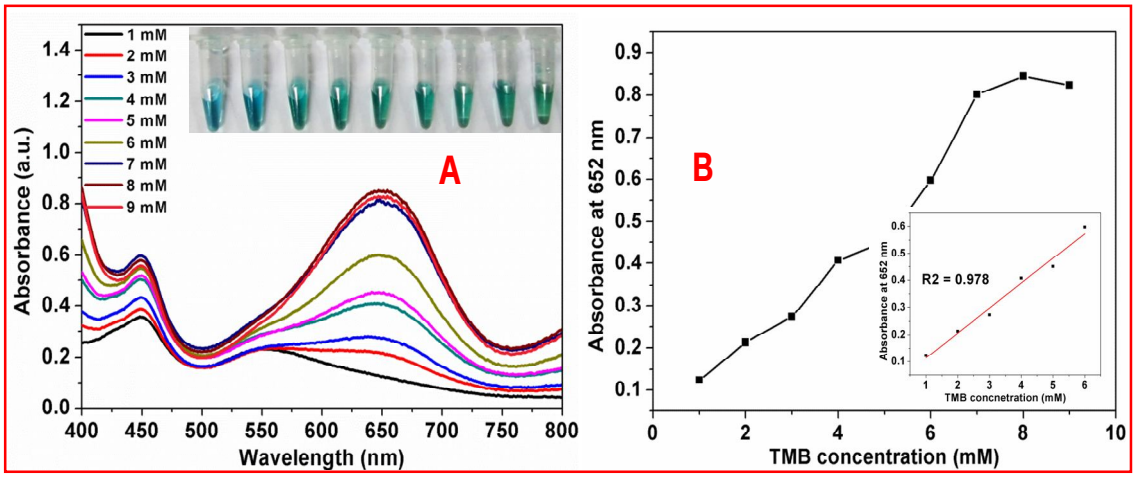

Figure 5.13 Peroxidase-like activity of NC-AuNPs at different (A) TMB concentrations from 1 mM to 9 mM using 50 µL of 1 mM H_2O_2 and 50 µL NC-AuNPs in 200 µL of 0.2 M NaAc buffer at constant pH 4 and temp 40 ^oC for 60 min with inset photograph showing the gradual change in color with the increase in TMB concentrations, (B) relationship between absorbance and TMB concentration with inset calibration plot showing the linear relationship between 1 – 6 mM TMB with R^2 = 0.978

Figure 5.13A showed the effect of different concentration of TMB from 1 mM to 9 mM which revealed that the intensity of the UV-visible spectra increased with the increase in TMB concentration upto 7 mM. On further increasing the TMB concentration, no significant increase in intensity was observed. The **Inset Figure 5.13A** also strengthened the above fact by showing the gradual increase in color intensity. Therefore, 7 mM was considered as optimum TMB concentration using 50 µL H_2O_2 of 0.5 mM and 50 µL NC-AuNPs in 200 µL 0.2 M NaAc buffer. The relationship between absorbance and TMB concentration is shown

in **Figure 5.13B** with inset calibration plot showing the linear relationship between 1 - 6 mM TMB with $R^2 = 0.978$.

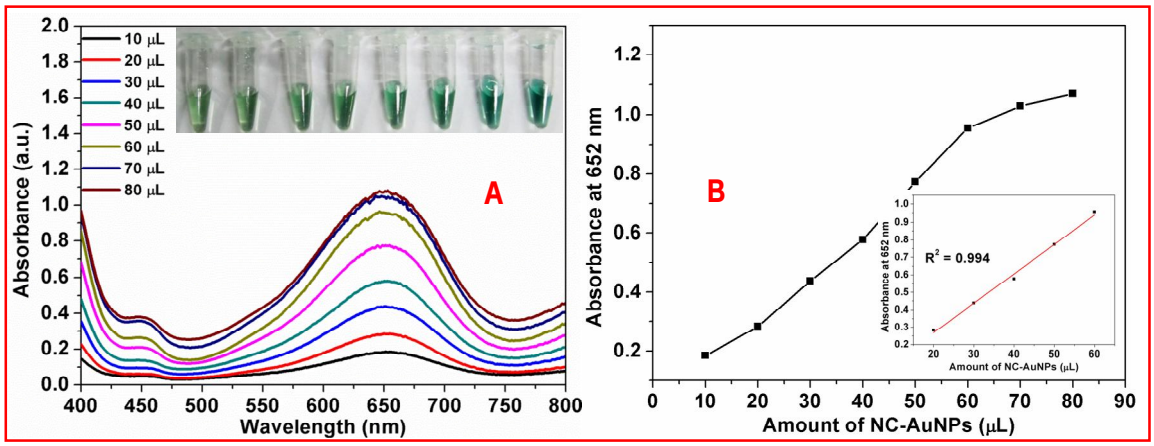

Figure 5.14 Peroxidase-like activity of NC-AuNPs at different (A) NC-AuNPs amount from 10 µL to 80 µL using 50 µL H_2O_2 of 0.5 mM and 50 µL TMB of 7 mM in 200 µL of 0.2 M NaAc buffer at constant pH 4 and temp 40 ^oC for 60 min with inset photograph showing the gradual change in color with the increase in NC-AuNPs amount, (B) relationship between absorbance and NC-AuNPs amount with inset calibration plot showing the linear relationship between 10 µL to 90 µL with $R^2 = 0.994$

Similarly, the amount of NC-AuNPs was also optimized using same set of experiments and found that too high or too low amount of NC-AuNPs was not suitable for the better peroxidase-like activity of NC-AuNPs. While optimizing the NC-AuNPs, it was observed that 70 µL NC-AuNPs was optimum for the better peroxidase-like activity at 50 µL TMB of 7 mM and 50 µL H_2O_2 of 0.5 mM in 200 µL of 0.2 M NaAc buffer (**Figure 5.14A)**. **Inset Figure 5.14A** was in accordance with the UV-visible spectra which corroborated the corresponding change in color. **Figure 5.14B** showed the relationship between absorbance and NC-AuNPs amount with inset calibration plot which revealed the linear relationship between 20 µL - 60 µL NC-AuNPs with $R^2 = 0.994$.

5.3.6 Detection of H_2O_2

After the optimization of different process parameters, the detection of H_2O_2 was carried out. For the detection purpose, different concentrations of H_2O_2 ranging from 0.025 mM to 0.200 mM were added into the optimized reaction system containing 70 µL NC-AuNPs and 50 µL TMB of 7 mM in 200 µL of 0.2 M NaAc buffer at constant pH 4 and temp 40 ^oC. **Figure 5.15A** revealed that as the concentration of H_2O_2 increased, the color and the intensity of UV-visible spectra also increased which was also in accordance with the change in color of the reaction system (**Inset Figure 5.15A**). The calibration plot of change in absorbance versus the H_2O_2 concentration at 652 nm showed the linear relationship between 0.025 mM to 0.150 mM with regression coefficient (R^2) = 0.997. The calculated standard deviation (SD) was found to be 0.0095 and the limit of detection (LOD) was 0.007 mM i.e. 7 µM which was calculated using SD and slope (B = 4.01) of the calibration curve (**Figure 5.15B**) according to the formula: LOD=3(SD/B). The limit of detection thus obtained was satisfactory with the previously reported results **Table 5.1**.

Table 5.1 comparison table showing the peroxidase-like activity of different nanomaterials for the colorimetric detection of H_2O_2

Nanomaterials	Substrate	Detection limit (µM)	Linear range	Reference
Co_3O_4 NPs	TMB	10	50-25000	Mu *et al*. 2013
$AgVO_3$	TMB	5	75-250	Xiang *et al*. 2016
$Cu_2(OH)_3Cl$-CeO_2 composite	TMB	10	20-50	Wang *et al*. 2015
Co-Al	TMB	10	10-50	Chen *et al*. 2013
NC-AuNPs	TMB	7	25-125	Present work

It is important to note here that this is the first report on the peroxidase-like activity of NC-AuNPs synthesized form leaf extracts which showed it potential peroxidase like activity towards the colorimetric detection of H_2O_2.

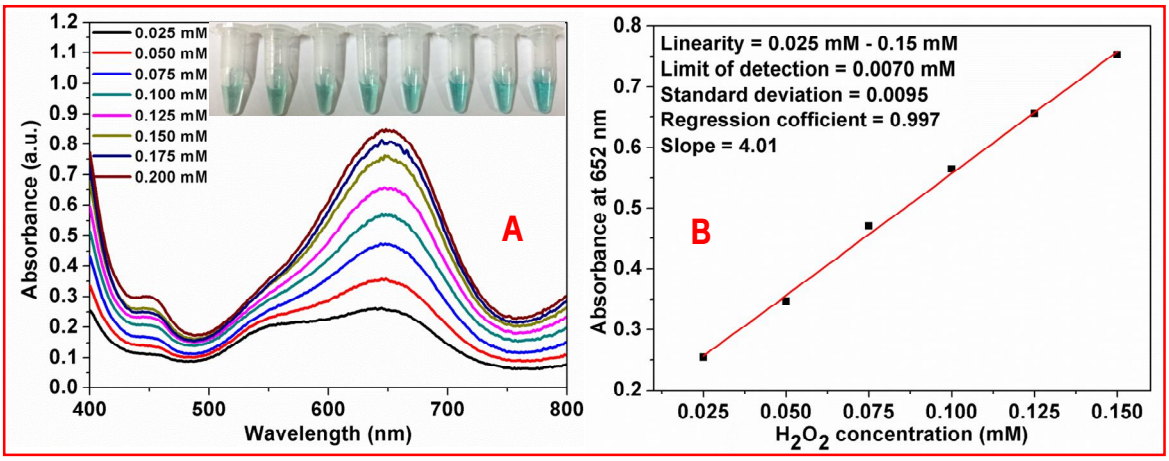

Figure 5.15 (A) Change in UV-visible absorbance spectra at different concentration of H_2O_2 from 0.025 mM to 0.200 mM using 80 µL NC-AuNPs and 50 µL TMB of 7 mM in 200 µL of 0.2 M NaAc buffer at constant pH 4 and temp 40 ^oC for 60 min with inset photograph showing the gradual change in color with the increase in H_2O_2 concentration, (B) the calibration plot of change in absorbance versus the H_2O_2 concentration at 652 nm showing the linear relationship between 0.025 mM to 0.150 mM with R^2 = 0.997 and LOD 0.028 mM

5.3.7 Selectivity

The selectivity of the NC-AuNPs was investigated by adding 100 µL of 1 mM of different possible interfering agents like ascorbic acid (AA), citric acid (CA), H_2O_2, glucose, and sucrose into the same reaction system used for the detection of H_2O_2. **Figure 5.15** revealed the corresponding absorbance of each interfering agents. The figure revealed that NC-AuNPs showed its highest selectivity for H_2O_2. Therefore, it was concluded that NC-AuNPs can be used for the selective colorimetric detection of H_2O_2.

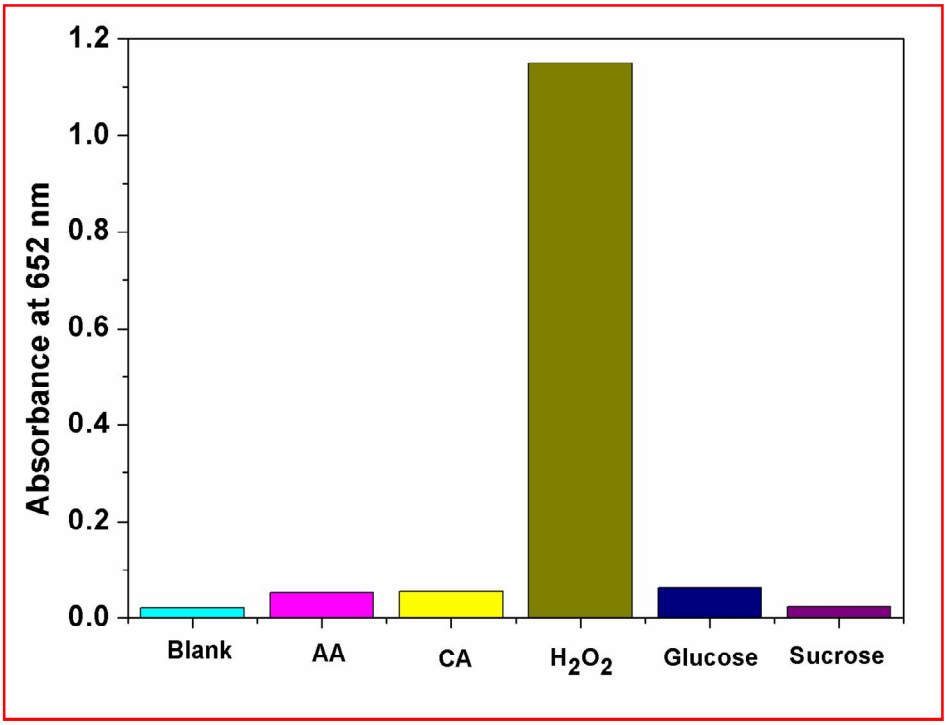

Figure 5.16 Selectivity test of NC-AuNPs using 50 µL of 1 mM each with AA (ascorbic acid), CA (citric acid), H_2O_2, glucose, and sucrose using 80 µL NC-AuNPs and 50 µL TMB of 7 mM in 200 µL of 0.2 M NaAc buffer at constant pH 4 and temp 40 ^oC for 60 min with inset photograph showing the corresponding change in color

5.4 Conclusion

The present study described the photoinduced green synthesis of AuNPs using AEX with different size and shape. The synthesis process was confirmed by the change in color of the reaction mixture and the development of sharp SPR band. The factors affecting the synthesis process such as sunlight exposure time, AEX inoculum dose and $HAuCl_4.xH_2O$ concentration were optimized using one parameter at a time approach which were 30 min, 3%, and 1.2 mM respectively. The effect of different concentration of $HAuCl_4.xH_2O$ on size was also investigated from 0.4 mM to 3.2 mM. The XRD analysis of the AuNPs synthesized from 0.4 mM to 3.2 mM showed diffraction peaks at $2\theta = 38.1^{\circ}$, 44.3°, 64.6° and 77.6°. The

peaks were well matched with (JCPDS) file no: 040784 and attributed to (111), (200), (220) and (311) Bragg reflections respectively. FTIR analysis advocated the important role played by phytochemicals in the synthesis and stabilization of AuNPs. The XPS analysis corroborated the presence of two individual peaks at 86.6 and 89.3 eV which corresponded to the presence of metallic gold. Zeta potential study revealed the synthesis of negatively charged AuNPs (NC-AuNPs) having zeta potential -7.4 mV. The NC-AuNPs depicted excellent peroxidase-like mimicking activity which was utilized for the colorimetric detection of hydrogen peroxide.